Frequency-Controlled Slip Speed Perception in a Dual-Array Tactile Display

by

Maarten Wooldrik

to obtain the degree of Master of Science
at the Delft University of Technology,
to be defended publicly on 26-05-2026 at 08h30.

Student number: 4557336
Thesis committee: dr. ir. A.H.A. Stienen, TU Delft, Committee Chair
dr. ir. M. Wiertlewski, TU Delft, Responsible Supervisor
L. Strakovsky, TU Delft, Daily Supervisor

TU Delft

Frequency-Controlled Slip Speed Perception in a Dual-Array Tactile Display

Maarten Wooldrik

***Abstract*—The sensation of tactile slip is ubiquitous to dexterous in-hand manipulation and plays a central role in grip control and surface perception. Replicating these sensations artificially is a valuable tool for increasing embodiment and immersion in robotic teleoperation and virtual reality applications. Existing slip-rendering devices span a wide range of designs, including vibrotactile, belt-, platform-, and tactor-based systems, each involving varying degrees of mechanical complexity. The present device elicits vivid tactile slip illusions through a minimalist architecture of only two independently actuated interleaved pin arrays [1], [2]. When driven in anti-phase, the arrays produce a differential motion mode that reliably evokes the sensation of a surface slipping beneath the finger. Building on this platform, the present work investigates whether vibration frequency can serve as an independent control parameter for perceived slip speed, independent of amplitude. A two-alternative forced-choice psychophysical experiment was conducted with 30 participants. In the motion detection part of the experiment, participants reliably identified the anti-phase stimulus as motion at 70 Hz and 90 Hz (both $p < .001$), while performance at 50 Hz did not exceed chance, attributed to hardware resonance. In the speed discrimination part of the experiment, participants consistently perceived frequencies above the 70 Hz reference as faster ($p < .001$ at 80 and 90 Hz), while four participants showed an inverted frequency–speed relationship. These results support frequency variation as a viable encoding strategy for perceived slip speed in dual-array tactile displays.**

***Index Terms*—Haptic interfaces, tactile displays, slip perception, vibrotactile feedback, vibration frequency encoding.**

I. Introduction

Tactile slip, the relative motion of an object surface against the skin of the fingertip, is a mechanically critical event in dexterous manipulation. When grasping an object, humans continuously regulate grip force to prevent object loss without applying excessive and potentially damaging force. Slip signals trigger rapid, reflexive grip force adjustments that maintain stable contact. Furthermore, controlled slip is actively used to reposition objects or reorient fingers without breaking contact [3]. The ability to detect and respond to slip is therefore a functional necessity for fine manipulation.

At the mechanistic level, slip perception arises from the activity of mechanoreceptors distributed across the glabrous skin of the fingertip, which respond to the spatiotemporal pattern of skin deformation during contact [4]. Four mechanoreceptor populations are relevant, each coupled to a distinct class of tactile afferent nerve fiber that carries signals from the receptor toward the central nervous system. Merkel discs are coupled to slowly adapting type I (SA1) afferents; they respond to sustained normal pressure and encode the spatial distribution of contact force. Ruffini endings are coupled to slowly adapting type II (SA2) afferents; they are sensitive to sustained skin stretch and the direction of tangential stress. Meissner corpuscles are coupled to fast adapting type I (FA1) afferents; they respond to the onset and offset of skin deformation and are particularly sensitive to low-frequency vibrations and slip events. Pacinian corpuscles are coupled to fast adapting type II (FA2) afferents; they are tuned to high-frequency vibrations and are activated by the rapid transients generated by microscale stick-slip events at the contact interface [5]. As a surface slides, local asperities alternately adhere to and release from the skin, also known as stick-slip events. These events generate a broadband vibration signal that collectively encodes the state of the sliding contact [6].

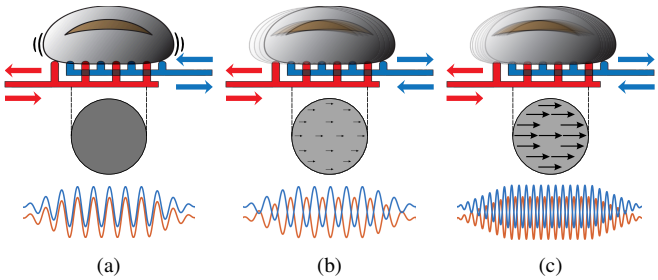

Fig. 1. **Dual array haptic display. (a)** In-phase actuation leads to the sensation of a vibrating surface. **(b)** Anti-phase actuation creates localized skin stretch events eliciting the sensation of slip. **(c)** Higher frequency anti-phase actuation elicits faster perceived slip speed. Figure inspired by Massalim *et al.* [1].

Dexterous manipulation under conditions where direct tactile feedback and information of these mechanoreceptors is unavailable presents a persistent and practically significant challenge. In robotic teleoperation, including applications in deep-sea exploration, remote surgery, nuclear decommissioning, and space robotics, operators must perform complex manipulation tasks through a remote manipulator without the benefit of natural hand contact [7], [8]. In most commercially deployed systems, tactile feedback is absent entirely, forcing operators to rely on visual feedback alone. Without tactile feedback, operators struggle to regulate contact forces appropriately, and object loss or unintended damage remain common issues in teleoperated tasks [8]. While sensor technology for detecting slip at the robot fingertip has advanced considerably, the complementary problem of reliably *displaying* that slip information to the human operator remains largely unsolved [9], [10].

A range of haptic interface designs have been proposed to

M. Wooldrik is with the Faculty of Mechanical Engineering, Delft University of Technology, 2628 CD Delft, The Netherlands. e-mail: m.wooldrik@student.tudelft.nl

address this gap, broadly classifiable into vibrotactile devices, global skin stretch devices, and localized pin-array stimulators. Vibrotactile approaches are compact and widely deployed but can be unnatural, distracting, and uncomfortable over long periods of use [11]. Furthermore, existing vibrotactile devices often lack directional specificity required for slip rendering [12]. Global skin stretch devices, including belt-driven [13], [14], platform-driven [15], [16], and tactor-driven designs [17], [18], act more directly on the mechanoreceptors responsible for shear detection and have demonstrated measurable reductions in grip force errors when slip feedback is provided. However, whilst effective for precise, directional slip feedback at a high spatial resolution, these devices are often very bulky and complex, and most importantly require high precision motor control. Localized pin-array displays can in principle reproduce spatially resolved contact mechanics, but the requirement for independent actuation of each contact point leads to systems that are mechanically complex, power-intensive, and poorly suited to wearable or teleoperation-compatible form factors [19], [20].

Beyond the question of whether slip is occurring, the *speed* of slip carries additional information: faster slip implies more rapidly deteriorating contact conditions and demands a proportionally larger or faster corrective response. Additionally, reliably translating slip speed will only further improve the transparency of teleoperated systems and therefore increase the operators sense of embodiment. Conveying not just the occurrence, but also the speed of slip to a remote operator, is therefore an important open problem. However, across all device categories described above, experimental validation of perceived slip *speed* as distinct from slip direction or distance is notably absent.

Gross slip is accompanied by micro-scale stick-slip events whose spectral content scales with sliding speed. Greenspon *et al.* demonstrated that as a textured surface is scanned across the fingertip at increasing speeds, the frequency composition of the resulting skin vibrations shifts systematically toward higher frequencies while skin displacement amplitude remains approximately constant [21]. At the neural level, Delhaye *et al.* showed that Pacinian corpuscle afferents, which are most sensitive to high-frequency vibrations, are the dominant carriers of speed information in the peripheral nerve, and that their firing rate is the best single predictor of perceived speed across both speed and texture conditions [22]. Together, these findings identify vibration frequency as a primary sensory cue for slip speed perception.

This raises a practical question: can a haptic display exploit this frequency-speed relationship to render perceived slip speed directly? Massalim, Faux, and Hayward proposed a dual-array tactile display that addresses the broader rendering problem with a mechanically minimal design, reducing the actuation problem to just two degrees of freedom: two interleaved 10×13 pin arrays, each driven by a single actuator, arranged in a quincunx configuration, illustrated schematically in Fig. 1 [1]. By controlling the phase relationship ϕ between the arrays, the device tunes the balance between two modes of motion. The common-mode motion, expressed by $s_{\text{com}} = \cos(\phi/2)\sin(\omega t)$, replicates whole-surface vibration and creates the sensation of a vibrating surface, as depicted in Fig. 1a. The differential-mode motion, expressed by $s_{\text{diff}} = \sin(\phi/2)\cos(\omega t)$, produces the spatially non-uniform lateral skin deformation characteristic of a finger sliding on a rough surface, depicted schematically in Fig. 1b. Anti-correlated motion was shown to produce significantly stronger perceived intensity than correlated motion at equal physical amplitude, with perceived intensity nearly twice that of the common-mode condition for broadband waveforms.

A subsequent study extended these findings by combining large-amplitude common-mode triangular motion with small-amplitude differential-mode noise, producing a vivid directional illusion of tactile slip despite zero net displacement. In doing this, the authors demonstrated that perceived slip distance scales with differential-mode amplitude [2]. This establishes the dual-array architecture as a mechanically simple yet perceptually rich platform for slip rendering. However, two important gaps remain. First, whether participants perceive the anti-phase stimulus as motion or slip per se, rather than merely as a more intense vibration, has not been directly tested. Second, perceived slip speed has only been modulated through changes in amplitude; whether varying vibration frequency can independently modulate perceived slip speed has not been investigated.

The present study addresses both of these open questions using the dual-array platform as its experimental device. A two-part psychophysical experiment was conducted with 30 participants. The Motion Detection experiment directly tested whether the anti-phase stimulus evokes a motion perception, independent of amplitude cues. The Speed Discrimination experiment tested whether varying differential-mode frequency independently modulates perceived slip speed, with amplitude held constant across conditions. The hypothesis that high-frequency anti-phase vibration elicits faster perceived motion is schematically depicted in Fig. 1c. The remainder of this paper presents the device (Section II), the experimental methodology (Section III), the results (Section IV), and a discussion of their implications for haptic interface design as well as the design limitations of the present study (Section V).

II. Device

The present device, shown in Fig. 2, is a dual-array vibrotactile display built on the working principle introduced by Massalim *et al.*, described in Section I [1]. It consists of two independently actuated interleaved pin arrays, a custom transconductance amplifier circuit, and an arbitrary waveform generator, all mounted on a rigid aluminum optical breadboard. The following sections describe each subsystem in turn.

A. Mechanical Design

The display comprises two arrays of pins arranged in a quincunx configuration and stacked such that the pins of the lower array protrude through through-holes in the upper array, with all pins terminating in the same plane. The complete array spans 36 mm $\times$ 29.25 mm and contains 115 pins in total. The pins are 1.5 mm in diameter, with lengths of 10 mm and 20 mm for the upper and lower arrays respectively; the lower

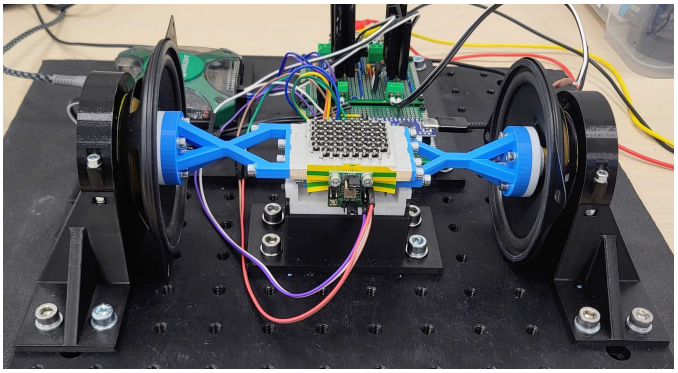

(a)

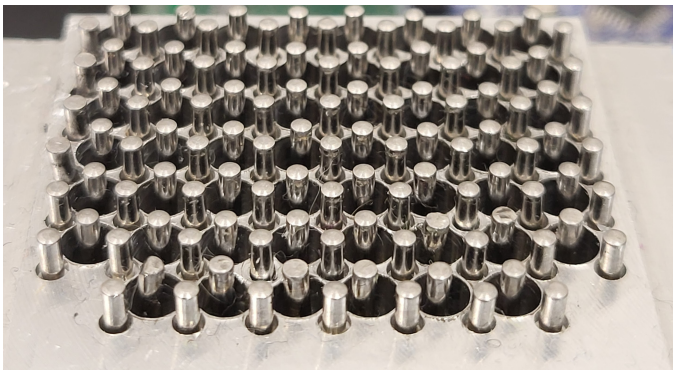

(b)

Fig. 2. **Dual array haptic display. (a)** Two broadband speakers actuate two suspended interleaved pin arrays. **(b)** The stainless steel pins are arranged in a quincunx formation.

array pins protrude through 4 mm diameter clearance holes. All pins are DIN 7 dowel pins, precision-machined from A1 stainless steel and individually press-fitted into the arrays. The arrays themselves were machined from 5754 aluminum alloy. This choice was made to maximize rigidity and mass, in an attempt to minimize the system's resonance frequency.

Each array is independently suspended by a four-flexure mechanism designed to provide low stiffness in the transverse planar direction, the direction of stimulation, and high stiffness in all other directions. This was done to ensure that actuation forces are transmitted efficiently to the skin without parasitic motion. A close-up view at the suspension can be seen in a modeled version of the device in Fig. 3b. The flexures were manufactured from spring steel strips of dimension 5 mm × 19 mm × 0.1 mm. Both pin arrays are actuated by two inverted

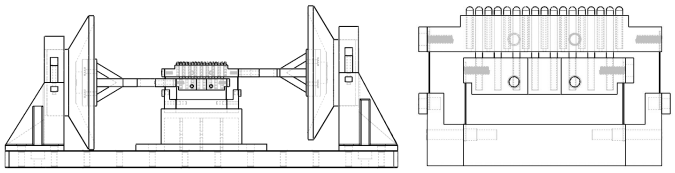

(a) (b)

Fig. 3. **3D Model of the mechanical system. (a)** Side view of the entire mechanical system. **(b)** Close-up of the pin arrays and flexures. Transmission and base parts removed for clarity.

broadband loudspeakers, each rated at 20 W, coupled to their respective arrays via custom 3D-printed transmission parts. Additional mounting hardware was also 3D-printed, and the complete assembly was secured to a 300 mm × 300 mm × 12.7 mm solid aluminium breadboard. A 3D model of the full system can be seen in Fig. 3a.

B. Actuation and Electronics

Loudspeaker voice coils are inherently inductive loads whose impedance rises with frequency, meaning that a conventional voltage amplifier would deliver progressively less current, and therefore less force, as frequency increases. Furthermore, back-EMF generated by coil motion introduces velocity-dependent feedback that distorts the relationship between the input signal and the resulting mechanical output. Because the Laplace force acting on the coil is directly proportional to current rather than voltage, the most straightforward solution is to drive the coil with a current source. The speakers were therefore driven by a voltage-controlled transconductance amplifier, which presents high input impedance to the signal generator, preventing loading effects on the waveform source. This amplifier converts the command voltage into a proportional output current regardless of the coil's impedance or back-EMF. This ensures that the Laplace force is directly proportional to the command voltage u across the full operating frequency range of the device.

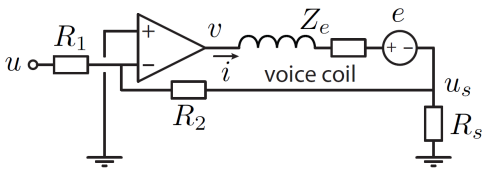

Fig. 4. **Transconductance amplifier circuit.**

The circuit design was inspired by the coil drive described by Wiertlewski and Hayward [23], shown schematically in Fig. 4. The amplifier was built around an OPA548 operational amplifier (Texas Instruments, Dallas, TX, USA) with feedback provided by a precision shunt resistor R_s, giving a transconductance gain of

$$\frac{i}{u} = -\frac{R_2}{R_1 R_s} \tag{1}$$

The component values were selected based on the operating constraints of the system. The waveform generator produces output voltages in the range 0 – 5 V, with an average operating amplitude of approximately 2.5 V. To avoid thermally overloading the amplifier board, the output current was limited to a maximum of 1.5 A, which at the average command voltage gives a required gain of magnitude $1.5\,\mathrm{A}/2.5\,\mathrm{V} = 0.6\,\mathrm{A\,V^{-1}}$. The amplifier was powered by ±12 V bench supplies, providing sufficient voltage headroom above the expected load voltage to prevent output saturation across the operating frequency range. With $R_1 = 10\,\mathrm{k\Omega}$, $R_2 = 3.3\,\mathrm{k\Omega}$, and $R_s = 0.5\,\Omega$, the resulting transconductance gain is $-0.66\,\mathrm{A\,V^{-1}}$, closely matching the design target. The amplifier circuit was mounted

directly on the breadboard alongside the signal generation hardware.

C. Frequency Response

The complete mass-spring oscillator formed by each array and its flexure suspension has a natural frequency of approximately 42 Hz. The frequency response was measured in an unloaded condition using two analogue MEMS accelerometers (ADXL356, Analog Devices, Wilmington, MA, USA), one mounted on each array, with data captured at 100 kSa/s using a digital storage oscilloscope (InfiniiVision DSOX2014A, KeySight, Santa Rosa, CA, USA). The measured response is shown in Fig. 5. A secondary resonance peak is visible at approximately 85 Hz. The resonance at 42 Hz is relevant to the interpretation of experimental results at 50 Hz. During those trials, the proximity to the natural frequency produces elevated and potentially distorted vibration amplitudes relative to higher frequency conditions. This point is further discussed in Section V. The non-flat frequency response means that a constant-amplitude command signal would produce unequal mechanical output across the experimental frequencies. Amplitude correction was therefore applied to equalize the physical displacement delivered at each test frequency.

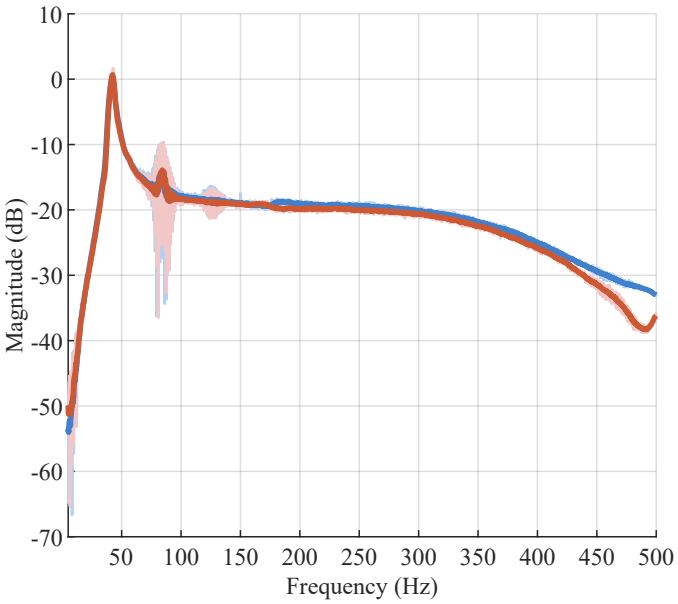

Fig. 5. **Frequency response of the device.** The system behaves as a mass-spring oscillator with a natural frequency of approximately 42 Hz and a secondary resonance peak at approximately 85 Hz.

D. Signal Generation

Waveforms were generated using the Python API of an Arbitrary Waveform Generator (Analog Discovery 2, Digilent, National Instruments, Austin, TX, USA), which provided independent two-channel output with programmable amplitude, frequency, and phase. This allowed the phase relationship ϕ between the two arrays to be set precisely for each experimental condition, enabling direct control of the common-mode and differential-mode motion as described in Section I. To ensure equal mechanical output across all test frequencies, despite the non-flat frequency response, a feedforward amplitude correction was applied. The correction gain at each frequency was determined empirically in a loaded condition: the command amplitude was adjusted until the peak displacement measured by the accelerometers was equalized across all stimulus frequencies, independently for each array. This per-frequency amplitude table was then applied consistently across all experimental trials. The exact waveforms used in the experiment will be discussed in Section III. An overview of the pipeline showing each component of the system can be seen in Fig. 6.

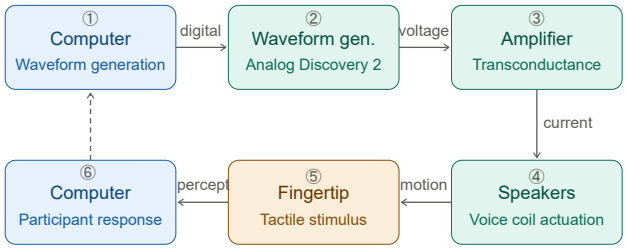

Fig. 6. **System pipeline.** Waveforms are generated in software and output via an arbitrary waveform generator (Analog Discovery 2), converted to a proportional current by a transconductance amplifier, and delivered to two loudspeaker voice coils which actuate the pin arrays. The resulting tactile stimulus is perceived by the participant, who reports their response via a keyboard, closing the experimental loop.

III. Methods

A. Experimental Design

A two-part psychophysical experiment was conducted to address the two research questions motivating this thesis. The Motion Detection experiment examined whether the phase difference between the two pin arrays influences the perception of motion. While Massalim *et al.* demonstrated that anti-phase stimulation produces stronger perceived intensity and a directional slip illusion, direct empirical evidence that participants perceive the anti-phase stimulus specifically as *motion*, rather than merely as a more intense vibration, was absent [1], [2]. The Motion Detection experiment was designed to fill this gap. The Speed Discrimination experiment examined whether differential-mode frequency independently modulates the perceived speed of this motion.

Both parts used a two-interval forced-choice (2-IFC) paradigm, in which participants were presented with two sequential stimuli per trial, and asked to indicate which one corresponded to a target perception. The 2-IFC was chosen for its simplicity and robustness: it does not require participants to assign an absolute rating to a sensation, which is cognitively demanding and subject to large individual variation. Instead, it leverages the relative judgment that humans make naturally and reliably [24]. The order in which the stimuli were presented was randomized on a trial-by-trial basis. The two parts were conducted sequentially with a two-minute rest between them.

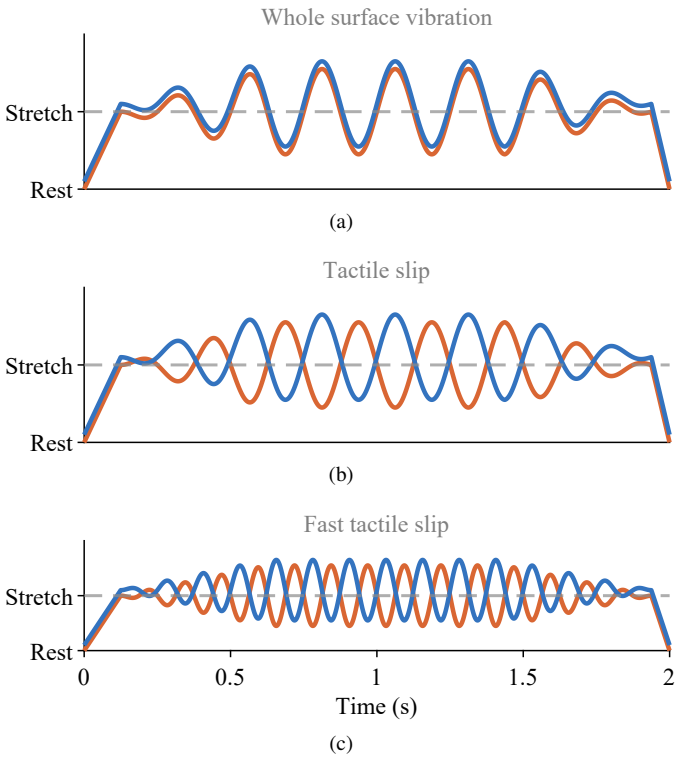

Fig. 7. **Stimulus waveforms.** All stimuli start with a common mode motion illustrated in the figure by a linear increase in amplitude at the beginning of each signal. This shift creates a lateral stretch of the fingerpad, before differential mode begins. **(a)** In-phase differential mode elicits a whole surface vibration. **(b)** Anti-phase differential mode elicits a perception of relative motion, or slip. **(c)** The frequency of the differential mode signal is varied to alter the perceived speed of the motion. Higher frequencies are hypothesized to be perceived as faster, and lower frequencies as slower.

B. Stimuli

All stimuli consisted of a sinusoidal signal with a superimposed DC offset ramp and an amplitude envelope, applied simultaneously to both pin arrays. The stimulus design was motivated by the mechanics of real frictional slip.

At the onset of each stimulus, both arrays were displaced *in phase* by a linearly increasing DC offset, rising from 0 V to 1.6 V over 0.125 s. This in-phase displacement, referred to hereafter as the common-mode displacement, produces a lateral pre-load of the finger pad skin via global tangential shear across the entire contact area. This shift is mechanically similar to the loading phase that precedes gross slip in natural object manipulation. This primes the skin before the differential-mode sinusoidal component is introduced.

The sinusoidal component was then introduced gradually via a trapezoidal amplitude envelope with a rise time of 0.5 s and a fall time of 0.5 s, surrounding a steady-state period of 0.8125 s. The gradual amplitude onset was intended to simulate the progressive recruitment of stick-slip events across the contact area as the finger transitions from full stick to fully developed sliding. While individual micro-slip events are mechanically abrupt (discrete asperities release very suddenly), it is hypothesized that the envelope of collective vibration amplitude at the contact interface builds progressively during this transition. An instantaneous onset would be inconsistent with this physical process [25]. In real sliding contact, the transition from stick to gross slip involves a progressive increase in the spatial extent and intensity of micro-slip events across the contact area, spreading from the contact periphery to the center of the contact area [26]. While the present stimulus does not replicate this spatial progression, since all pins are driven simultaneously, the temporal amplitude envelope approximates the gradual build-up of vibration intensity that accompanies the onset of sliding. A similar frequency sweep envelope was considered to further simulate slip acceleration, but not implemented, as traversing the system's natural frequency of 42 Hz during a stimulus produced perceptual artifacts. At stimulus offset, the common-mode displacement was reversed over 0.0625 s. Each stimulus had a total duration of 2 s. The resulting waveform is illustrated in Fig. 7.

The sinusoidal waveform used here is a deliberate simplification. Physically realistic frictional slip generates broadband vibrations with a $1/f$ spectral profile arising from the random micro-scale stick-slip events at the contact interface [6]. A pink noise signal of this kind was initially considered for use in the present study, following the approach of Massalim *et al.* [2]. However, the loudspeaker actuators used in the present device were not capable of reproducing pink noise at a displacement amplitude sufficient to produce a clearly perceptible sensation. At the amplitudes required, the acoustic output of the speakers during noise playback was also judged too loud and qualitatively different from sinusoidal conditions, risking that participants would use auditory rather than tactile cues to distinguish stimuli, even through noise-cancelling headphones. A sinusoidal signal was therefore chosen as a reliable alternative. Critically, the use of a single-frequency sinusoid also made it possible to calibrate stimulus amplitude independently at each test frequency more easily, something that would not have been straightforward with a broadband signal. There, the overall amplitude and spectral shape would interact with the device's non-flat frequency response in more complex ways.

The phase relationship between the two arrays distinguished the two stimulus types used in the Motion Detection experiment. In the *in-phase* condition ($\phi = 0°$), both arrays moved synchronously, producing whole-surface vibration without differential skin deformation. In the *anti-phase* condition ($\phi = 180°$), the arrays moved in anti-phase, producing localized lateral skin stretch, hypothesized to elicit a motion perception. These two extremes were selected on the basis of Massalim *et al.*, who found the largest difference in perceived intensity between the fully correlated ($\phi = 0°$) and fully anti-correlated ($\phi = 180°$) conditions, making them the most likely to produce a detectable perceptual difference in a forced-choice task [1]. Intermediate phase values were not tested, as the primary goal of the Motion Detection experiment was to establish whether motion perception can be elicited at all, rather than to characterize its dependence on phase.

C. Procedure

1) Motion Detection: In the Motion Detection experiment, participants were presented with pairs of stimuli; one *in-phase* and one *anti-phase*, and asked to indicate which they

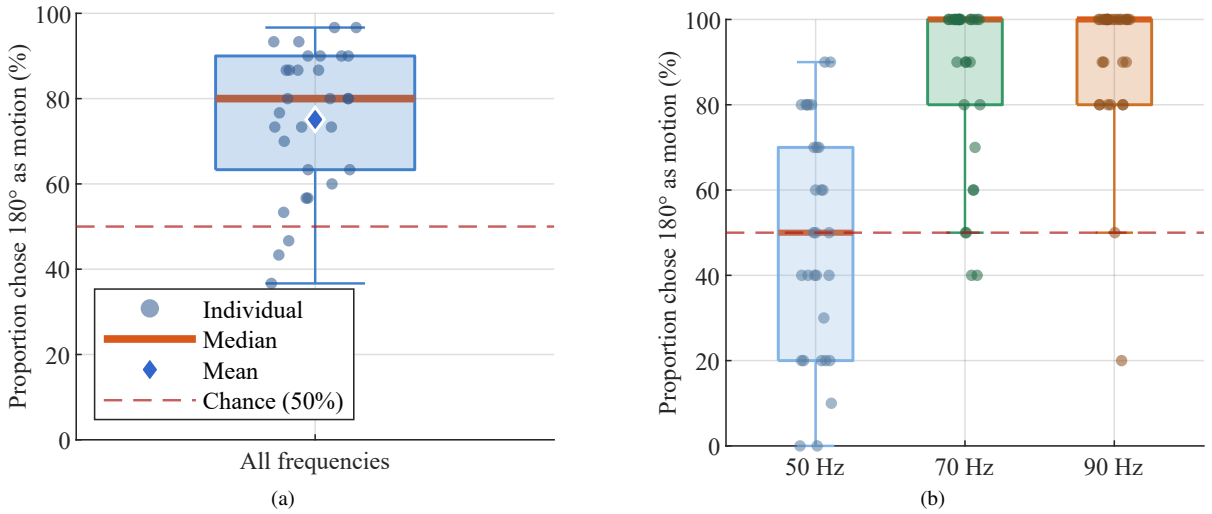

Fig. 8. **Phase-dependent motion perception. (a)** Participants reliably identified 180° anti-phase stimulation as motion (M = 75%, $p < .001$). **(b)** Detection accuracy varied by frequency, with near-chance performance at 50 Hz but robust detection at 70 Hz and 90 Hz, indicating a frequency threshold for the illusion.

associated most with motion. The phase conditions were tested at three frequencies: 50 Hz, 70 Hz, and 90 Hz. Each frequency was tested ten times in randomized order, resulting in 30 trials per participant.

2) Speed Discrimination: In the Speed Discrimination experiment, all stimuli were anti-phase ($\phi = 180°$), and only frequency was varied. Participants were asked to indicate, keeping the sensation of motion from the previous experiment in mind, which of two stimuli felt like the faster motion. A fixed reference frequency of 70 Hz was compared against four test frequencies: 50 Hz, 60 Hz, 80 Hz, and 90 Hz. Each comparison was repeated ten times in randomized order. Two catch trials, in which both stimuli were presented at 70 Hz, were included to monitor response bias. This resulted in 42 trials per participant.

D. Participants

Thirty healthy participants (15 female, 15 male, mean age = 25.2 years, SD = 2.3, range 22–31), were recruited and provided written informed consent prior to participation. Participants were informed of the general nature of the task but were not told the specific research hypotheses to avoid influencing their answers. Each participant rested their right index finger on the device, wore noise-canceling headphones playing broadband masking noise to prevent auditory cues from the device, and made responses via a graphical user interface. Pin array motion was in the medial-lateral direction. The full experiment lasted approximately 15–20 minutes per participant.

IV. Results

A. Motion Detection

Across all 30 participants and all frequency conditions, the proportion of trials in which participants chose the *anti-phase* stimulus as the one perceived as motion had a mean of .75 ($SD = .17$, median $= .80$), as seen in Fig. 8a. A Shapiro-Wilk test indicated that the overall distribution deviated from normality ($W = 0.925$, $p = .036$), so a one-tailed Wilcoxon signed-rank test was used to assess whether the group proportion exceeded chance. The result was significant ($W = 452$, $p < .001$), confirming that the anti-phase differential-mode stimulus reliably elicited a motion perception across the sample. To examine whether this effect held at each frequency, one-tailed tests were conducted per condition, with the choice between parametric and non-parametric determined by Shapiro-Wilk normality tests. The results of this analysis can be seen in Fig. 8b.

At 50 Hz, the data were normally distributed ($W = 0.943$, $p = .111$) and a one-sample t-test showed the mean proportion of .49 ($SD = .27$) was not significantly above chance ($t(29) = -0.27$, $p = .606$). At 70 Hz, the distribution deviated significantly from normality ($W = 0.718$, $p < .001$), and a Wilcoxon signed-rank test showed the mean proportion of .86 ($SD = .20$) was significantly above chance ($W = 401$, $p < .001$). At 90 Hz, the distribution was similarly non-normal ($W = 0.588$, $p < .001$), and the mean proportion of .90 ($SD = .18$) was also significantly above chance ($W = 431$, $p < .001$). A one-way repeated-measures ANOVA revealed a significant effect of frequency on the proportion of trials in which participants identified the motion stimulus ($F(2, 58) = 52.18$, $p < .001$). Post-hoc pairwise t-tests with Bonferroni correction ($\alpha = .0167$) showed significant differences between 50 Hz and 70 Hz ($t(29) = -7.64$, $p < .001$) and between 50 Hz and 90 Hz ($t(29) = -7.45$, $p < .001$), but no significant difference between 70 Hz and 90 Hz ($t(29) = -1.76$, $p = .090$). The notably lower performance at 50 Hz is not attributed to a difference in perceptual mechanism; a potential hardware-related explanation for this finding will be addressed in Section V.

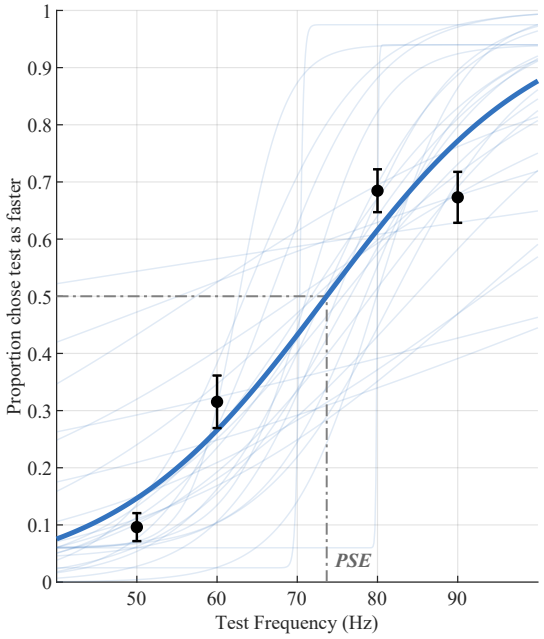

Fig. 9. **Effect of Frequency on Speed Perception.** Psychometric curves show the proportion of trials where participants chose the test frequency as feeling faster than the 70 Hz reference. Four outlying participants were excluded from the analysis due to misinterpretation of the task. Individual fits (shown here as thin blue lines) reveal substantial variability in how frequency maps onto perceived slip speed. The group mean curve (thick blue line) shows no systematic bias (PSE = 75.2 Hz, $p = .114$). Black markers with error bars represent mean ± SEM across participants.

B. Speed Discrimination

Prior to the main analysis of the speed discrimination part of the psychophysical experiment, four participants with divergent behavior were excluded on the basis of a negative psychometric slope ($k < 0$), indicating that they perceived higher frequencies as *slower* rather than faster. While this pattern runs counter to the hypothesized direction of the frequency–speed relationship, it represents a genuine and theoretically interesting perceptual response that will be addressed in Section V. The remaining 26 participants all showed a positive slope, consistent with the hypothesis that higher differential-mode frequency is associated with faster perceived slip speed.

For these 26 participants, the group mean PSE was 75.2 Hz ($SD = 16.1$ Hz, median $= 74.2$ Hz). A Shapiro-Wilk test indicated that the PSE distribution deviated from normality ($W = 0.910$, $p = .028$), so a two-tailed Wilcoxon signed-rank test was used to assess whether the group PSE differed from the 70 Hz reference. The result was significant ($W = 254$, $p = .046$), indicating that the group PSE was systematically shifted above the reference frequency.

To assess whether participants reliably perceived individual test frequencies as faster than the 70 Hz reference, one-tailed tests were conducted on the proportion of trials in which participants chose each test frequency as faster, tested against chance level (0.5). Shapiro-Wilk tests guided the choice of parametric or non-parametric test per condition. At 50 Hz and 60 Hz, proportions of .10 ($SD = .13$) and .32 ($SD = .23$) were not significantly above chance, indicating these frequencies were perceived as *slower* than the reference (both $p > .99$). At 80 Hz, the distribution was normal ($W = 0.940$, $p = .137$) and the proportion of .69 ($SD = .19$) was significantly above chance ($t(25) = 4.92$, $p < .001$). At 90 Hz, the distribution was also normal ($W = 0.941$, $p = .144$) and the proportion of .67 ($SD = .23$) was likewise significantly above chance ($t(25) = 3.88$, $p < .001$). These results demonstrate a systematic effect of differential-mode frequency on perceived slip speed, with frequencies above the 70 Hz reference reliably perceived as faster.

As an exploratory post-hoc analysis, the 80 Hz and 90 Hz proportions were directly compared using a paired t-test. The two did not differ significantly ($t(25) = 0.30$, $p = .765$), indicating that the effect of frequency on perceived speed did not increase further between 80 Hz and 90 Hz.

Individual PSE estimates ranged widely across participants, with values spanning from 30.0 Hz to 110.0 Hz (mean 75.2 Hz, $SD = 16.1$ Hz, median 74.2 Hz), as seen in Fig. 10a. The distribution of PSEs was right-skewed, driven by a small number of participants whose estimates approached the boundary of the tested frequency range. The significant upward shift of the group PSE relative to the 70 Hz reference suggests a mild but consistent tendency for participants to require a test frequency somewhat above the reference before perceiving it as faster, indicating a slight perceptual bias favoring the reference stimulus.

Fig.10b shows the slope parameter k, which quantifies the precision of frequency discrimination: participants with steeper slopes showed a more abrupt transition from choosing the reference to choosing the test stimulus as faster, while shallower slopes reflect more gradual, less certain discrimination. Among the 26 participants included in the slope analysis, k ranged from 0.005 Hz^{-1} to 0.343 Hz^{-1} (median 0.081 Hz^{-1}, $M = 0.098\ \text{Hz}^{-1}$, $SD = 0.076\ \text{Hz}^{-1}$), indicating substantial individual variability in sensitivity to frequency differences. Two excluded participants, whose slopes exceeded 1 Hz^{-1}, represent cases of near-perfect discrimination and were only excluded from the figure for clarity.

V. Discussion

The present study investigated two open questions in tactile slip rendering using a dual-array haptic display: whether anti-phase differential-mode stimulation reliably evokes the perception of motion, and whether vibration frequency can independently modulate perceived slip speed. The results provide affirmative evidence for both questions, with important nuances that are discussed below.

A. Motion Detection

The group-level finding that anti-phase stimulation was reliably identified as the motion stimulus ($p < .001$) was supported by qualitative responses collected from participants after the experiment. The large majority described the Motion Detection experiment as intuitive and straightforward. Several participants reported sensing a directional quality to the anti-phase stimulus, describing it as feeling 'pushed' in a particular direction or as their finger sliding along a textured surface.

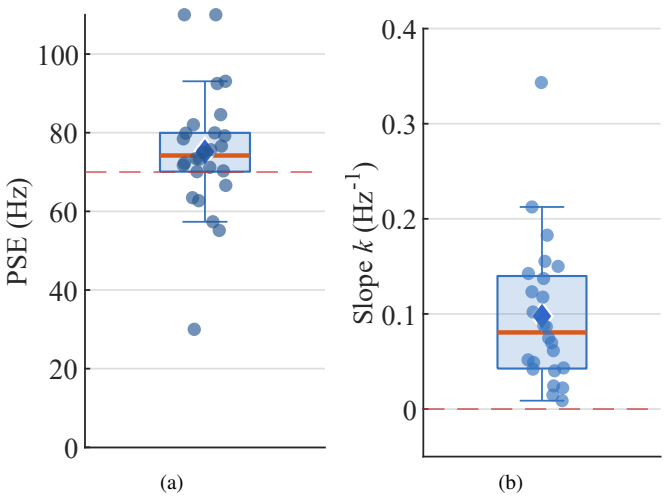

Fig. 10. **Fitted parameter distribution.** The dots represent individual results, and the diamond marker the mean result. The median result is illustrated with the full orange line in both graphs. **(a)** Distribution of the Point of Subjective Equality (PSE; $n = 26$), representing the test frequency at which each participant was indifferent between the test and 70 Hz reference stimulus. The dashed red line marks the reference frequency. **(b)** Distribution of the psychometric slope k (Hz^{-1}; $n = 24$), reflecting the steepness of frequency discrimination around the PSE. Two participants with extreme slope estimates ($k > 1$ Hz^{-1}) are excluded from this panel for scaling purposes but retained in all other analyses. The dashed red line marks zero, corresponding to no frequency sensitivity.

Several participants described the sensation as resembling slip or sliding specifically, while others noted characteristics consistent with slip, such as discrete skin stretch events, or a sense of movement relative to the surface, without labeling it as slip per se. Notably, even participants who did not spontaneously describe the sensation as slip reported a clear and systematic perceptual difference between the two stimulus types, suggesting that the perceptual effect is robust to individual differences in how participants interpret or verbalize tactile sensations.

B. Speed Discrimination

Turning to the Speed Discrimination experiment, results revealed a significant effect of differential-mode frequency on perceived slip speed at the group level, with frequencies above the 70 Hz reference reliably perceived as faster ($p < .001$ at both 80 Hz and 90 Hz), and frequencies below the 70 Hz reference not perceived as faster (both $p > .99$). Participant comments reflected the added difficulty of the task relative to the Motion Detection experiment: most described speed discrimination as more challenging than motion detection, and a number reported uncertainty about the cue they were using, noting it was sometimes difficult to separate the sensation of higher frequency from that of faster movement. Nonetheless, a majority of participants reported that higher frequencies did feel faster, and the psychometric analysis supports this at the group level.

A post-hoc direct comparison between the 80 Hz and 90 Hz proportions confirmed that the two did not differ significantly ($t(25) = 0.30$, $p = .765$), suggesting a perceptual plateau above approximately 80 Hz. This plateau could reflect saturation at the level of the mechanoreceptor populations engaged by the differential-mode stimulus, such that further increases in frequency no longer produce a distinguishable change in perceived speed. Alternatively, it may reflect a ceiling in the perceptual mapping between frequency and speed rather than a somatosensory limitation: participants may simply lose the ability to translate higher frequencies into a faster motion perception once frequency exceeds a certain value, regardless of receptor firing rates. Verbal comments from several participants noted that the motion sensation felt more pronounced at lower frequencies, suggesting that the strength of the motion perception itself is also frequency-dependent.

C. Individual Differences

In the Motion Detection experiment, there were no clear outliers in the same sense as the Speed Discrimination experiment: only three participants scored at or below chance overall (P03 at 37%, P20 at 47%, P27 at 43%), and of these, the low scores were largely driven by near-chance performances at 50 Hz. At this frequency, resonance-induced amplitude elevation likely distorted the stimulus and hampered the ability to perceive a clear difference between in-phase and anti-phase stimulation. At 70 Hz and 90 Hz, the vast majority of participants reliably identified the anti-phase stimulus as motion, indicating that the perceptual effect is robust when the stimulus is delivered outside the resonance region. The group of participants who reported some ambiguity are likely explained by differences in the conceptual interpretation of 'motion' rather than a failure to perceive the anti-phase stimulus. Verbal reports suggest that some participants interpreted "which stimulus do you associate with motion?" as referring to gross finger movement, rather than relative motion between the pins and the skin. Under this interpretation, the in-phase stimulus, which produces larger global displacement and thus more whole-finger vibration, might systematically be chosen. Participants who interpreted the question in terms of relative or surface motion showed a clear preference for the anti-phase stimulus, and the task was well understood by the vast majority.

In the Speed Discrimination experiment, individual differences were much more pronounced. Four participants showed a negative psychometric slope, perceiving higher frequencies as slower rather than faster. Unlike the ambiguity in the Motion Detection experiment, these inversions are not attributable to the resonance issue alone: the inverted frequency-speed relationship persisted across the full range of tested frequencies, suggesting a fundamentally different cue strategy. The most plausible explanation is that these participants weighted amplitude rather than frequency as their primary speed cue. Because the amplitude calibration was not individually personalized, inter-frequency amplitude differences may have been present at the participant level. As a result, a participant experiencing higher amplitude at 50 Hz than at 90 Hz might rationally judge the former as faster. The frequency dependence of the motion perception itself may have further contributed: the illusion is known to vary in strength across the tested frequency range. A participant who perceived the low-frequency stimulus as

more vivid may have interpreted that greater intensity as an indication of faster motion, rather than using frequency as the speed-cue. These four participants serve as a reminder that frequency is not the only cue available in this task, and that in natural sliding contact, slip speed perception is not driven by frequency alone. Vibration amplitude, intensity, contact area, surface texture, and friction all contribute [21]. Individual differences in cue weighting therefore represent a genuine source of variability that is not captured by the group-level psychometric analysis.

D. Limitations

Two catch trials per participant, in which both stimuli were presented at the 70 Hz reference frequency, were included in the Speed Discrimination experiment to monitor response bias. However, a data recording error resulted in the trial order not being saved correctly, making it impossible to identify whether the chosen stimulus was the first or second interval presented. As a result, potential response biases such as a systematic tendency to choose the second stimulus, which several participants mentioned spontaneously, could not be quantified or corrected for. This is a notable limitation, as an undetected order bias could have systematically altered the responses of individual participants.

A further source of uncontrolled variability is the device's frequency response. The device has a natural frequency of approximately 42 Hz, and the 50 Hz test condition falls within the resonance region. As a result, the physical displacement amplitude at 50 Hz was elevated relative to other test frequencies, even after the amplitude calibration described in Section III. The root cause is that calibration was performed by a single experimenter who likely applied a higher than average normal contact force, resulting in a smaller resonance-induced displacement than a typical participant. Participants with lighter touch would therefore have experienced a disproportionately high amplitude at 50 Hz. This could potentially have driven the near-chance performance in the Motion Detection experiment and the systematic perception of 50 Hz as faster in the Speed Discrimination experiment. A more robust approach would be to perform amplitude calibration individually for each participant under a standardized contact force. Furthermore, neither normal force nor finger displacement were actively monitored during the experiment, meaning that inter-participant variability in contact mechanics could not be controlled or measured.

Alternatively, three design directions could mitigate the resonance issue in future iterations. First, increasing the mass of the pin arrays or reducing the stiffness of the flexure suspension could help lower the natural frequency below 20 Hz and free the lower end of the actuation spectrum of artifacts. Second, an attempt could be made to achieve the opposite; create a relatively high resonance peak by using substantially light and stiff material. This would put the operating range well below the system's natural frequency and would require less powerful actuators than in the previous solution. Finally, the system could benefit from an active damping component to suppress the resonance peak without changing the fundamental architecture, at the cost of a more complex design.

A further limitation of the present study is associated with the semantics of the question asked during the experiment. The Motion Detection experiment asked participants to indicate which stimulus they 'associated with motion', rather than which felt like slip. This wording was deliberately chosen to avoid biasing participants toward a specific perceptual label, since asking 'which feels like slip?' presupposes that either stimulus feels like slip at all. However, this comes at the cost of precision: several participants described the perception in ways consistent with gross vibration rather than relative surface motion. Verbal reports suggest the directional component of the slip perception is present but weak, which is consistent with the common-mode displacement being insufficient to produce a strong directional skin pre-load at the amplitudes used.

Several adaptations could be made to solidify the perception of slip. Stronger actuation allowing a larger common-mode displacement would likely enhance the directional quality of the stimulus. However, in the current design, much of the common-mode displacement might be absorbed by whole finger and wrist movement. An attempt to mitigate this was made by grounding the participants' wrists to a stable surface, but this would still not necessarily isolate the finger. An alternative approach to validate the slip perception would be to have participants slide their finger over an actual textured surface and match that sensation to the device stimulus, directly grounding the perception in real slip experience.

Similarly, the Speed Discrimination experiment asked which stimulus felt like 'the faster motion'. A fundamental ambiguity is whether participants were genuinely perceiving a change in the speed of the motion illusion, or simply detecting a higher frequency and associating that directly with speed. Several participants noted this explicitly in their verbal comments. The partial mitigation was to conduct the Motion Detection experiment first, establishing the motion perception before the speed discrimination task, so that participants would have a reference for the motion sensation when making speed discrimination judgments. Whether this was sufficient to fully decouple speed perception from raw frequency detection cannot be determined from the present data.

Finally, prolonged vibrotactile stimulation is known to produce mechanoreceptor adaptation, leading to a reduction in sensation intensity and, at high sustained amplitudes, numbness or tingling [27]. The present experiment lasted 15–20 minutes and involved discrete vibrotactile stimulation throughout, with only a two-minute rest between parts. Several participants reported a tingling or mildly numb sensation in the fingertip following the experiment. While the randomized trial order distributed adaptation effects across conditions, a more systematic mitigation would have been to have participants briefly engage in non-vibrotactile finger activity between trials to facilitate mechanoreceptor recovery, or incorporate longer rest periods between blocks.

E. Frequency as a Control Parameter

The present results establish that differential-mode frequency modulates perceived slip speed within a meaningful

range, but also reveal its limits as a standalone parameter. The motion perception itself is frequency-dependent: changes in frequency intended to encode speed simultaneously alter the strength and quality of the motion illusion. A truly independent frequency-speed mapping would require the perceptual quality of the illusion to remain constant as frequency varies, which the present device does not achieve across its operating range. Future work should examine whether varying frequency as well as amplitude (increasing frequency while maintaining a constant motion percept strength), can decouple these two perceptual dimensions more effectively.

It is important to note that in the present study, the common-mode displacement was held constant in amplitude and slope across all test conditions. This was a deliberate design choice to isolate the effect of differential-mode frequency on perceived slip speed. This ensured that any difference in speed perception between conditions could be attributed to frequency alone rather than to differences in the common-mode stimulus. However, the common-mode displacement itself is a natural parameter for encoding speed: a steeper ramp corresponds to a faster simulated transition from stick to slip, and increasing its slope would be expected to enhance the perceived speed of the slip event. Future designs could therefore exploit all three parameters simultaneously; differential-mode frequency, differential-mode amplitude, and common-mode ramp slope and duration, to produce a richer encoding of perceived slip speed.

F. Future Directions

The present findings establish a perceptual proof of concept for the dual-array architecture, while mapping out clearly what remains to be solved before it can be deployed in practice. Miniaturization is a central requirement: the current device, mounted on a rigid aluminum breadboard with external amplifiers, is far from wearable, but remote actuation approaches where the actuators are located off-hand and force is transmitted via tendons or cables, could substantially reduce the end-effector size.

The effect of the slip illusion in combination with visual feedback, as experienced in a teleoperation or virtual reality context, is unknown and may significantly alter the perceptual outcome; congruent visual and tactile cues tend to enhance each other, and the current device has only been tested in isolation [28].

A two-display configuration, with two devices placed facing away from each other, would allow the slip illusion to be delivered to both the thumb and index finger simultaneously, more closely approximating the tactile input during real pinch grasping. It can then be investigated whether this configuration improves grip force adjustments in a teleoperation task, when slip is signaled. The addition of a force sensor beneath the pin arrays would allow grip force responses to be measured directly in response to the slip stimulus, closing the loop between tactile display and motor behavior.

What remains is to test whether these perceptual effects translate into real task benefits, whether an operator actually adjusts grip force faster, drops fewer objects, or performs more confidently when the slip illusion is present.

VI. Conclusion

This work set out to address two specific gaps in the tactile slip rendering literature. The first was an absence of direct empirical evidence that anti-phase stimulation from a dual-array display is perceived as motion, as opposed to merely a more intense vibration. The second was an open question about whether vibration frequency can serve as an independent control parameter for perceived slip speed, without changes in amplitude. Both questions were addressed through a psychophysical experiment with 30 participants, using a 2-IFC paradigm.

The results answer both questions affirmatively. Anti-phase stimulation at 70 Hz and 90 Hz was reliably perceived as motion by the large majority of participants, with many spontaneously describing the sensation in terms consistent with slip or directional surface movement. Differential-mode frequency was shown to modulate perceived slip speed: frequencies above the 70 Hz reference were consistently judged as faster, and lower frequencies as slower. These findings establish that a dual-array haptic display can encode perceived slip speed by varying vibration frequency alone, holding amplitude constant.

These results are a proof of concept rather than a complete solution. Several limitations were identified: the resonance of the device at 42 Hz distorted results near 50 Hz; amplitude calibration was not individualized; and the motion perception, while present, lacked the strong directional quality that would make it unambiguously felt as slip by all participants. Four participants in the Speed Discrimination experiment showed an inverted frequency-speed relationship, most likely due to using amplitude rather than frequency as their speed cue. This finding supports the knowledge that frequency is not the only perceptual dimension available in this task. Future devices should address resonance through mechanical redesign, and future experiments should pair the display stimulus with actual sliding contact to anchor the perceptual label more precisely.

The broader implication of this work sits at the intersection of perception science and haptic engineering. The sense of touch, and slip perception in particular, is the missing link in most current teleoperation and haptic rendering systems. Operators of remote manipulators, surgical robots, and deep-sea systems, routinely perform fine manipulation tasks without any tactile feedback, relying on vision to detect contact failures that the biological hand would resolve in milliseconds through reflexive grip force adjustment. The dual-array architecture demonstrated here offers a mechanically simple solution toward bridging this gap: two actuators, two pin arrays, and a controlled phase and frequency relationship are sufficient to elicit a convincing slip perception. The simplicity of this approach is what makes it practically relevant. More complex systems with higher actuator counts or multi-axis motion may achieve greater perceptual fidelity, but they come at the cost of miniaturization, latency, reliability, and ease of integration into wearable or practical form factors.

What remains to be demonstrated is whether the perceptual effect translates into behavioral benefit in a closed-loop manipulation task. The key experiment is straightforward in principle: deliver the slip illusion to an operator performing a

grasp-and-hold task with a teleoperated gripper, and measure whether grip force adjustments occur faster and more appropriately than without tactile feedback. If the answer is yes, then the dual-array architecture can become a practical component of a teleoperation system. The present work provides the perceptual foundation on which that experiment can be built.

REFERENCES

[1] Y. Massalim, D. Faux, and V. Hayward, "Distributed tactile display with dual array design," *IEEE Transactions on Haptics*, vol. 16, no. 2, pp. 334–338, 2023.

[2] Y. Massalim, D. Faux, V. Hayward, and H. Jörntell, "An illusion of tactile slip," *Multisensory Research*, p. 1–8, 2025.

[3] R. S. Johansson and G. Westling, "Signals in tactile afferents from the fingers eliciting adaptive motor responses during precision grip," *Experimental Brain Research*, vol. 66, no. 1, pp. 141–154, 1987.

[4] R. S. Johansson and Å. B. Vallbo, "Tactile sensory coding in the glabrous skin of the human hand," *Trends in Neurosciences*, vol. 6, pp. 27–32, 1983.

[5] R. S. Johansson and G. Westling, "Roles of glabrous skin receptors and sensorimotor memory in automatic control of precision grip when lifting rougher or more slippery objects," *Experimental Brain Research*, vol. 56, no. 3, pp. 550–564, 1984. [Online]. Available: https://doi.org/10.1007/BF00237997

[6] M. Wiertlewski, C. Hudin, and V. Hayward, "On the 1/f noise and non-integer harmonic decay of the interaction of a finger sliding on flat and sinusoidal surfaces," in *2011 IEEE World Haptics Conference*, 2011, pp. 25–30.

[7] C. Pacchierotti and D. Prattichizzo, "Cutaneous/tactile haptic feedback in robotic teleoperation: Motivation, survey, and perspectives," *IEEE Transactions on Robotics*, vol. 40, pp. 978–998, 2024. [Online]. Available: https://dx.doi.org/10.1109/tro.2023.3344027

[8] T. Li, Y. Yan, C. Yu, J. An, Y. Wang, and G. Chen, "A comprehensive review of robot intelligent grasping based on tactile perception," *Robotics and Computer-Integrated Manufacturing*, vol. 90, 2024. [Online]. Available: https://www.scopus.com/inward/record.uri?eid=2-s2.0-85195202570&doi=10.1016%2fj.rcim.2024.102792&partnerID=40&md5=a25e932557b142c25a0137c1c777fdb5

[9] G. Vitrani, B. Pasquale, and M. Wiertlewski, "Shadowtac: Dense measurement of shear and normal deformation of a tactile membrane from colored shadows," in *2025 IEEE International Conference on Robotics and Automation (ICRA)*, 2025, pp. 5004–5010.

[10] R. S. Johansson and J. R. Flanagan, "Coding and use of tactile signals from the fingertips in object manipulation tasks," *Nature Reviews Neuroscience*, vol. 10, no. 5, pp. 345–359, 2009. [Online]. Available: https://doi.org/10.1038/nrn2621

[11] S. Okamoto, M. Konyo, and S. Tadokoro, "Vibrotactile stimuli applied to finger pads as biases for perceived inertial and viscous loads," *IEEE Transactions on Haptics*, vol. 4, no. 4, pp. 307–315, 2011.

[12] Z. F. Quek, W. R. Provancher, and A. M. Okamura, "Evaluation of skin deformation tactile feedback for teleoperated surgical tasks," *IEEE Transactions on Haptics*, vol. 12, no. 2, pp. 102–113, 2019.

[13] K. Minamizawa, S. Fukamachi, H. Kajimoto, N. Kawakami, and S. Tachi, "Gravity grabber: wearable haptic display to present virtual mass sensation," in *ACM SIGGRAPH 2007 Emerging Technologies*, ser. SIGGRAPH '07. New York, NY, USA: Association for Computing Machinery, 2007, p. 8–es. [Online]. Available: https://doi-org.tudelft.idm.oclc.org/10.1145/1278280.1278289

[14] C. Pacchierotti, G. Salvietti, I. Hussain, L. Meli, and D. Prattichizzo, "The hring: A wearable haptic device to avoid occlusions in hand tracking," in *2016 IEEE Haptics Symposium (HAPTICS)*, 2016, pp. 134–139.

[15] R. Baavour, M. Fuchs, and U. Ben-Hanan, "Grip-slip: A slip/shear tactile display master unit for grip tasks," in *2007 Mediterranean Conference on Control and Automation, MED*, 2007, Conference Proceedings. [Online]. Available: https://www.scopus.com/inward/record.uri?eid=2-s2.0-50249162576&doi=10.1109%2fMED.2007.4433881&partnerID=40&md5=a9697c4df9dda913f4ba415756aab660

[16] M. J. Kim and A. Bianchi, "Spinocchietto: A wearable skin-slip haptic device for rendering width and motion of objects gripped between the fingertips," in *UIST 2022 Adjunct - Adjunct Proceedings of the 35th Annual ACM Symposium on User Interface Software and Technology*, 2022, Conference Proceedings. [Online]. Available: https://www.scopus.com/inward/record.uri?eid=2-s2.0-85141422284&doi=10.1145%2f3526114.3558651&partnerID=40&md5=14b24580f66ba054696817086520ec1d

[17] N. G. Tsagarakis, T. Horne, and D. G. Caldwell, "Slip aestheasis: A portable 2d slip/skin stretch display for the fingertip," in *Proceedings - 1st Joint Eurohaptics Conference and Symposium on Haptic Interfaces for Virtual Environment and Teleoperator Systems; World Haptics Conference, WHC 2005*, 2005, Conference Proceedings, pp. 214–219. [Online]. Available: https://www.scopus.com/inward/record.uri?eid=2-s2.0-84934284532&doi=10.1109%2fWHC.2005.117&partnerID=40&md5=fe22f9471efbfa96aeeb14d4d0a8dac5

[18] R. J. Webster, T. E. Murphy, L. N. Verner, and A. M. Okamura, "A novel two-dimensional tactile slip display: Design, kinematics and perceptual experiments," *ACM Transactions on Applied Perception*, vol. 2, no. 2, pp. 150–165, 2005. [Online]. Available: https://www.scopus.com/inward/record.uri?eid=2-s2.0-33750949348&doi=10.1145%2f1060581.1060588&partnerID=40&md5=5cdc802816bb3656cd4120db6b911823

[19] Q. Wang and V. Hayward, "Compact, portable, modular, high-performance, distributed tactile transducer device based on lateral skin deformation," in *2006 14th Symposium on Haptic Interfaces for Virtual Environment and Teleoperator Systems*, 2006, pp. 67–72.

[20] ——, "Tactile synthesis and perceptual inverse problems seen from the viewpoint of contact mechanics," *ACM Trans. Appl. Percept.*, vol. 5, no. 2, May 2008. [Online]. Available: https://doi-org.tudelft.idm.oclc.org/10.1145/1279920.1279921

[21] C. M. Greenspon, K. R. McLellan, J. D. Lieber, and S. J. Bensmaia, "Effect of scanning speed on texture-elicited vibrations," *Journal of The Royal Society Interface*, vol. 17, no. 167, p. 20190892, 6 2020.

[22] B. P. Delhaye, M. K. O'Donnell, J. D. Lieber, K. R. Mclellan, and S. J. Bensmaia, "Feeling fooled: Texture contaminates the neural code for tactile speed," *PLOS Biology*, vol. 17, no. 8, p. e3000431, 2019. [Online]. Available: https://dx.doi.org/10.1371/journal.pbio.3000431

[23] M. Wiertlewski and V. Hayward, "Transducer for mechanical impedance testing over a wide frequency range through active feedback," *Review of Scientific Instruments*, vol. 83, no. 2, p. 025001, 2012.

[24] F. A. Kingdom and N. Prins, *Psychophysics: A Practical Introduction*, 2nd ed. London: Academic Press, 2016.

[25] B. Delhaye, P. Lefèvre, and J.-L. Thonnard, "Dynamics of fingertip contact during the onset of tangential slip," *Journal of The Royal Society Interface*, vol. 11, no. 100, p. 20140698, 2014. [Online]. Available: https://doi.org/10.1098/rsif.2014.0698

[26] T. André, V. Lévesque, V. Hayward, P. Lefèvre, and J.-L. Thonnard, "Effect of skin hydration on the dynamics of fingertip gripping contact," *Journal of The Royal Society Interface*, vol. 8, no. 64, pp. 1574–1583, 04 2011. [Online]. Available: https://doi.org/10.1098/rsif.2011.0086

[27] S. J. Bensmaïa, Y. Y. Leung, S. S. Hsiao, and K. O. Johnson, "Vibratory adaptation of cutaneous mechanoreceptive afferents," *Journal of Neurophysiology*, vol. 94, no. 5, pp. 3023–3036, 2005.

[28] M. O. Ernst and M. S. Banks, "Humans integrate visual and haptic information in a statistically optimal fashion," *Nature*, vol. 415, no. 6870, pp. 429–433, 2002.